Int J Adv Manuf Technol (2016) 82:1079–1088
DOI 10.1007/s00170-015-7471-x

ORIGINAL ARTICLE

Investigation of chip formation and fracture toughness in orthogonal cutting of UD-CFRP

Hao Li[1] · Xuda Qin[1] · Gaiyun He[1] · Yan Jin[2] · Dan Sun[2] · Mark Price[2]

Received: 18 March 2015 / Accepted: 22 June 2015 / Published online: 30 June 2015

Abstract Features of chip formation can inform the mechanism of a machining process. In this paper, a series of orthogonal cutting experiments were carried out on unidirectional carbon fiber reinforced polymer (UD-CFRP) under cutting speed of 0.5 m/min. The specially designed orthogonal cutting tools and high-speed camera were used in this paper. Two main factors are found to influence the chip morphology, namely the depth of cut (DOC) and the fiber orientation (angle θ), and the latter of which plays a more dominant role. Based on the investigation of chip formation, a new approach is proposed for predicting fracture toughness of the newly machined surface and the total energy consumption during CFRP orthogonal cutting is introduced as a function of the surface energy of machined surface, the energy consumed to overcome friction, and the energy for chip fracture. The results show that the proportion of energy spent on tool-chip friction is the greatest, and the proportions of energy spent on creating new surface decrease with the increasing of fiber angle.

Keywords UD-CFRP · Orthogonal cutting · Fracture toughness · Chip formation

✉ Xuda Qin
qxd@tju.edu.cn

Hao Li
haolitju@tju.edu.cn

[1] Key Laboratory of Mechanism Theory and Equipment Design of Ministry of Education, Tianjin University, Tianjin 300072, China

[2] School of Mechanical and Aerospace Engineering, Queen University Belfast, Belfast BT9 5AH, UK

1 Introduction

Carbon fiber reinforced plastic (CFRP) composite consists of carbon fibers encapsulated by plastic matrix. The carbon fibers are responsible for carrying load, while the matrix serves to distribute, hold, and protect the fibers as well as to transmit the load [1–3]. This unique material structure contributes to the enhanced mechanical and structural properties and made CFRP an ideal substitute for metals. CFRP composites have many superior properties, such as high strength to weight ratio, excellent fatigue and creep resistance, low frictional coefficient, good toughness and damage tolerance, high wear and corrosion resistance as well as dimensional stability, and high vibration damping ability [4, 5]. Due to their superior properties, CFRP composites become very attractive in a variety of applications especially in the field of aerospace, aeronautical, and automotive industry. Components made from CFRP composites are mostly produced in near-net-shape. However, secondary manufacturing processes such as milling and drilling are often required for imparting the dimensional tolerances and assembly of composite parts [6–8].

Orthogonal cutting refers to the cutting process in which the tool edge is perpendicular to the direction of tool travel. Although it is uncommon in conventional industrial machining process, the operation provides an essential understanding of the deformation mechanism of machined CFRP materials. Machinability of CFRP mainly depends on the properties of fibers and matrix and their combined effects on chip formation mechanisms [9]. Koplev et al. [10] discussed the chip size and fracture with regard to fiber orientation using quasi-static orthogonal cutting tests of carbon/epoxy composites. Arola et al. [11] correlated chip formation mechanisms with fiber orientation and tool

geometry when orthogonally trimming graphite/epoxy composites using PCD tools. Chip formation was found to be predominately dependent on fiber orientation. Nayak et al. [12] have utilized the orthogonal cutting trials for inspecting the volume of material removed when machining glass/epoxy using HSS tool. Zitoune et al. [13] carried out similar experiments on unidirectional type of carbon/epoxy using the K20 carbide tool. It can be concluded from these reports that the machinability of CFRP is strongly dependent on the machining direction. When machining laminates with 0° fiber orientation, the compressive stress induced by the tool edge causes the fibers to break perpendicularly to their axes under buckling or bending. In classic fracture mechanics, the crack formation mechanism is divided into three modes. Mode I: external load is the normal stress which is perpendicular to the plane of crack, and the relative displacement of crack plane is perpendicular to the crack plane; mode II: external load is the shear stress which is perpendicular to the edge of crack and located in cracking plane. When machining laminates with fiber orientation $90° \leq \theta < 180°$ at a positive rake angle, mode I fracture initiates along the fiber-matrix interface causing delaminated material peel and slide on the rake face. When the fiber orientation is $0° \leq \theta < 90°$, mode II fiber failure occurs under compressive shear [6]. However, the influence of cutting parameters on chip morphology has not been elaborated in detail.

Cutting process models for composite materials have been developed over the past decades [14–18], and many of these models are based on the Merchant's single shear plane model [19], which was originally developed for metallic materials.

However, the CFRP cutting process is quite different as compared to metal cutting [20]. Several studies have adopted the Merchant shear plane theory for developing the constitutive approach. Everstine et al. [15] developed the first theoretical model on the cutting of FRP materials. The composite is treated as incompressible and inextensible along the fiber direction and the fibers are continuously distributed. The authors proposed a deformation field in the chip analogous to the field of the thick zone model with rupture and separation occurring ahead of the tool. Bhatnagar et al. [16] have presented an approach based on the Merchant theory and experimental validation on CFRP of fiber angle $0° \leq \theta < 90°$. In this model, the authors assumed the shear plane angle to be the fiber angle where failure occurs. Zhang et al. [17] developed a mechanical model to predict cutting forces during the orthogonal cutting of unidirectional FRP. For fiber orientations below 90°, the cutting zone has been divided into three regions: chipping, pressing, and bouncing. Jahromi et al. [18] developed an analytical model using elastoplastic matrix behavior to predict cutting forces during orthogonal cutting of unidirectional FRP ($90° \leq \theta < 180°$), and the authors distinguished three chip formation mechanisms: fiber bending, fiber microbuckling, and matrix shearing. And recently, the microscopic mechanism based on force prediction in orthogonal cutting of UD-CFRP was elaborated with analyzing the representative volume element [3]. However, due to the distinctively different material properties, it is difficult to accurately predict the failure and identify the chip formation mechanisms for composites, therefore, the new analysis method is required to better understand the material removal and chip formation processes for CFRP.

With the proposition and development of the fracture energy for newly generated surfaces, the cutting force balance model and energy conservation equation have been improved. Atkins [21] concluded that the work of fracture can be a significant component of total cutting work and established the cutting force equation by considering the surface energy as well as the plastic deformation in the primary shear zone and the friction along the tool-chip interface. Astokhov et al. [22] presented a methodology for practical estimation of cutting force and cutting power. Recently, Williams et al. [23] proposed a mechanical cutting methodology for the measurement of fracture toughness, and it is validated for several types of polymers. The approach is proven to be effective while avoiding the problems associated with crack blunting. However, to date, the analysis on fracture toughness and energy conservation has yet been developed for CRFP machining processes.

In this paper, detailed experimental investigation on UD-CFRP orthogonal cutting and chip formation mechanism are presented. The shear angle in orthogonal cutting with 0–75° fiber orientation has been obtained by examining the morphology feature of chipping region. A new method is introduced for measuring fracture toughness of newly machined CFRP based on the Williams model [23], which led to the formulation of the energy consumption model. Finally, the energy conservation analysis in the CFRP cutting process is also discussed in details.

2 Experiments

Fiber orientation angle is firstly investigated because of its great influence on chip formation in CFRP machining [16]. The fiber orientation angle, θ, is defined in Fig. 1. The tool feeding direction (cutting direction) is defined as the initial position (0°). When the tool rotates and coincides with the fiber orientation, the angle of rotation will be defined as the fiber orientation angle, θ. In this paper, the selected fiber angles were 0, 15, 30, 45, 60, 75, 90, 120, 135, and 150°.

The orthogonal cutting tests were carried out using specially designed cutting tools on a JOHNFORD (VMC-850) vertical machining center, as shown in Fig. 2. The tool

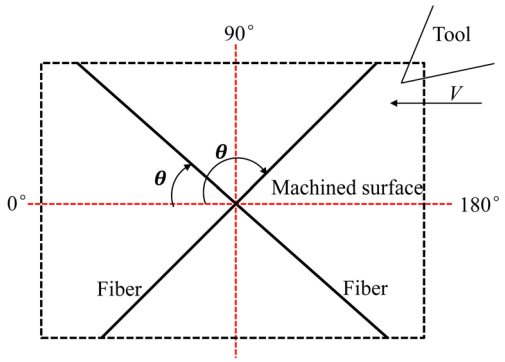

Fig. 1 Schematic definition of fiber angle θ in CFRP orthogonal cutting

matrix material is solid tungsten carbide (WC-8 %Co), and the cutting edge length is 7 mm which is greater than the workpiece thickness (5 mm), thus, the tool can effectively cut through the entire workpiece during orthogonal cutting process. The rake angle and clearance angle are 25° and 20°, respectively. Meanwhile, in order to ensure the sharpness of cutting edge, the tool is uncoated. The tool spindle was locked to ensure no rotational motion during the tests. Under the selected machine setting, the tool can only feed in the horizontal direction, and orthogonal cutting of different fiber orientations can be achieved by using different workpieces. The CFRP material was made from unidirectional prepreg with carbon fiber and epoxy resin matrix, and the material properties can be found in Table 1.

A Kistler three-direction stationary dynamometer (9257) with supporting Kistler charge amplifier (type 5070) was used, and data acquisition board and Kistler software were deployed for X and Y directions cutting force measurement. During the orthogonal cutting, high-speed camera images were captured at 500 pps. In order to obtain better quality images, a high power light source was used, shown in Fig. 2. The experimental condition has been defined following literature [12, 13, 24, 25] and details are listed in Table 2.

3 Experimental observation of chip formation

In CFRP, the ultimate strength of carbon fibers is much larger than that of the resin matrix, hence the fibers imposes most influence on the cutting process. Since carbon fiber belongs to elastic-brittle materials, its deformation during cutting is similar to other brittle materials. Different fiber orientation leads to anisotropic material properties, which in turn leads to different material deformation and chip formation mechanism. In CFRP cutting (especially for unidirectional CFRP), the cracking in workpiece always forms ahead of the cutting tool. Modes I and II are found to be the main crack propagation modes for CFRP orthogonal cutting process [6].

Depending on the fiber orientation, cutting process characteristics have been categorized into four types [26]: 0, 15–75, 75–90, and 90–180° fiber orientation. The analysis of chip formation in this study has also based on this classification.

3.1 Fiber angle θ = 0°

The images of chip formation at 0° fiber angle is shown in Fig. 3. It is clearly seen that the chip morphology is dependent on the DOC (a_c). When a_c = 0.1 mm (Fig. 3a, b), the chips are powder-like. Material crushing or peeling took place at the tool tip, leading to fiber bucking/bending fracture. For a_c = 0.5 mm (Fig. 4c, d), the crack forms and propagates along the fiber direction ahead of the tool. In other words, the tool is cutting on a surface that has already experienced bending and cracking. The DOC in this *second*

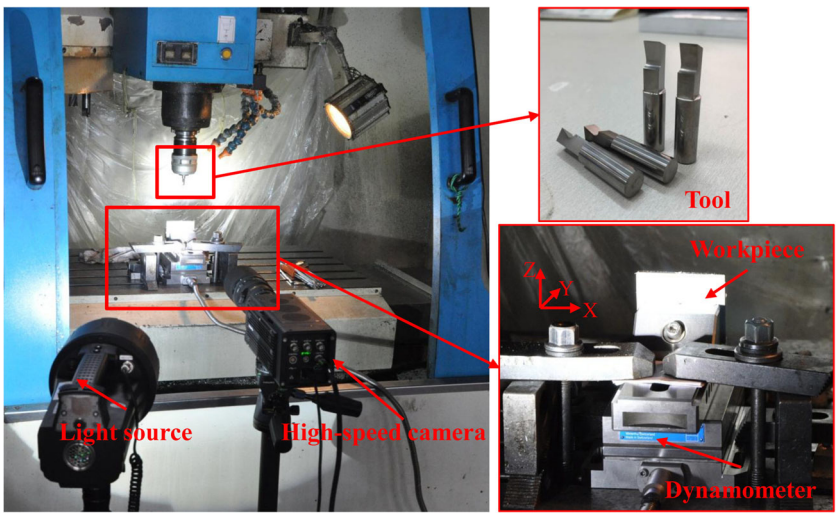

Fig. 2 Experimental set-ups of CFRP orthogonal cutting

Table 1 Material properties of T700/E765 epoxy resin matrix composites

Tensile strength, Yield	Tensile modulus	Compressive strength	Compressive modulus	Shear strength
2300 MPa	125 GPa	738 MPa	123 GPa	39.3 MPa

cut zone (red circle in Fig. 3d) was no longer 0.5 mm, but much shallower in the *second cut zone*.

As the tensile strength of the matrix (∼50MPa) is much lower than the compressive strength of the fiber, separation of the two phases occurs at the tool tip, and mode I fracture initiates along the fiber direction causing a layer of material to peel and to slide on the rake face. The tool continues to travel causing an increased bending stress on the peeled layer. The chip eventually breaks in direction perpendicularly to the fiber when the bending stress exceeds the bending limit of fiber, resulting in a blocky chip. Nevertheless, the powder-like chips were observed in the second cut zone, similar to what has been seen in Fig. 3a, b. The irregular powder-like chips consist of fiber and matrix powders resulting from the shear stress along the fiber direction (mode II fracture) and the materials buckling. The thickness of blocky chip (caused by mode I fracture) is dependent on DOC, and its length is dependent on the rake angle of the tools and the fiber bending stress.

3.2 Fiber angle $15° \leq \theta < 75°$

Figure 4 illustrates the chip formation process for $15° \leq \theta < 75°$. In this case, compression imposed by the cutting tool edge induced shear stress perpendicular to the axis of the fiber. When the shear stress exceeds the ultimate shear strength of carbon fiber, fiber fracture occurs. After that, the failed fiber slides along in the fiber direction under the compression induced by the cutting tool until a chip is formed (mode II fracture). Therefore, when the fiber orientation is $15° \leq \theta < 75°$ (only $\theta = 30°$ and $\theta = 60°$ shown in Fig. 4), micro-fracture occurs due to the compression-induced shear across the fiber axis and the interfacial shearing along the fiber direction, which eventually causes chip separation from the workpiece.

For this set of experiments, the DOC is also found having a significant influence on the morphology of chip. When the depth of cut is relatively low (a_c = 0.1 mm), the morphology of chips are continuous and ribbon-like, which turn into blocky when the depth of cut is 0.5 mm, as shown in Fig. 4. Unlike the continuous chip in metal machining, the continuous chip in CFRP orthogonal cutting is formed by weakly connected tiny chips which separate easily as the tool travels, as shown in Fig. 4c.

In the case of $15° \leq \theta < 75°$, the geometrical morphology of shear plane, i.e., the separation surface between chip and workpiece, was obtained using microscope with high resolution and depth of field. Due to the slip at the fiber/matrix interfaces, no fiber breakage was observed in shear plane, as shown in Fig. 5a. Based on the 3D coordinate value of shear zone under different fiber orientation, the value of shear angle for different Y position is obtained from trigonometric calculation. The mean shear angle corresponding to fiber angle 30, 45, and 60° were 28.6, 44.7, and 59.1°, respectively, as shown in Fig. 4b–d. The calculation results are closely coordinated with the corresponding fiber angles. Therefore, it can be concluded that chips are produced by shearing along the fiber direction and the shear angle can be substituted by fiber angle for $15° \leq \theta < 75°$. This is useful for analysis of fracture toughness in Section 4 of this paper.

3.3 Fiber angle $75° \leq \theta < 180°$

In the case of relatively high fiber orientation angle ($75° \leq \theta < 180°$), the chip is yielded due to bending under a severe compressive loading with an out-of-plane shear resulting in an inter-laminar deformation, as shown in Fig. 6a–c. Mode I fracture is not seen, whereas mode II occurs as soon as the tool comes into contact with the specimen [6]. The roughness of machined surface was poor due to the presence of the micro-cracks. Some of the bent fibers failed when the bending stress exceeds the yield strength of the fiber, and this mostly occurred below the cutting edge (cutting plane) where maximum stress occurs. Other bent fibers tend to bounce back, as shown in Fig. 6c, and this would degrade the quality of machined CFRP surface. Under this set of machining condition, the chip is continuous ribbon-like when a_c = 0.1 mm, and blocky chips were produced

Table 2 Experiment condition

Cutting speed (V)	Depth of cut (a_c)	Cutting width (a_w)	Cooling conditions
0.5 m/min	0.1, 0.2, 0.5 mm	5 mm	Dry

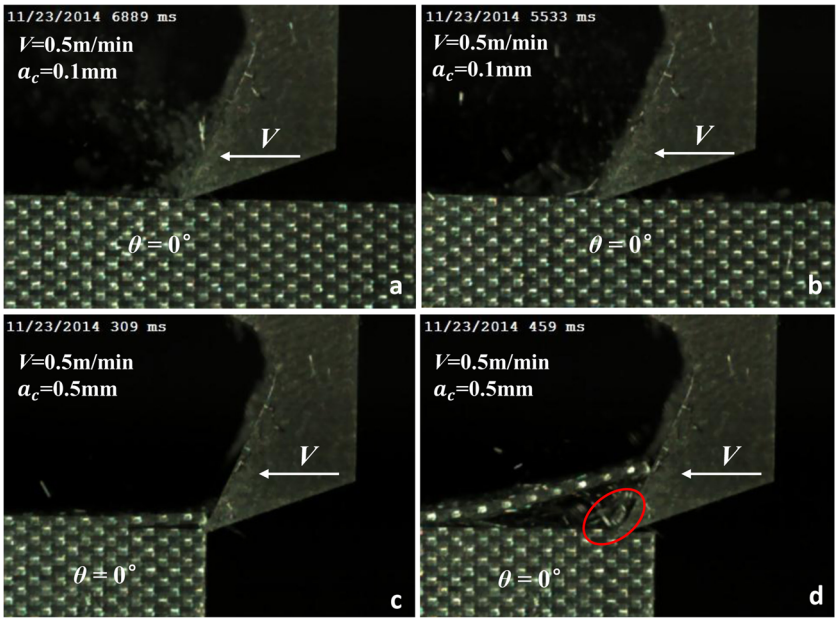

Fig. 3 Chip formation process in UD-CFRP orthogonal cutting ($\theta = 0°$)

when a_c = 0.2 mm. As shown in Fig. 6d, a catastrophic through crack was formed under a relatively larger DOC.

4 Fracture toughness and energy distribution

In the case of $15° \leq \theta < 75°$, the removed material undergoes shear yielding in the direction of fiber orientation when it moves along the tool rake face during orthogonal cutting process. In this case, the fracture occurs at the tool tip where the primary shear zone contacts with the bulk material. Figure 7 shows schematically the orthogonal cutting process where the geometric parameters of cutting zone and the cutting force between tool and chip are illustrated. The red dashed lines represents the chip separation surface in orthogonal cutting process.

As CFRP is a elastic-brittle material, and no plastic deformation takes place during the cutting process, the following equation applies,

$$a_{ch} = a_c, V_c = V \tag{1}$$

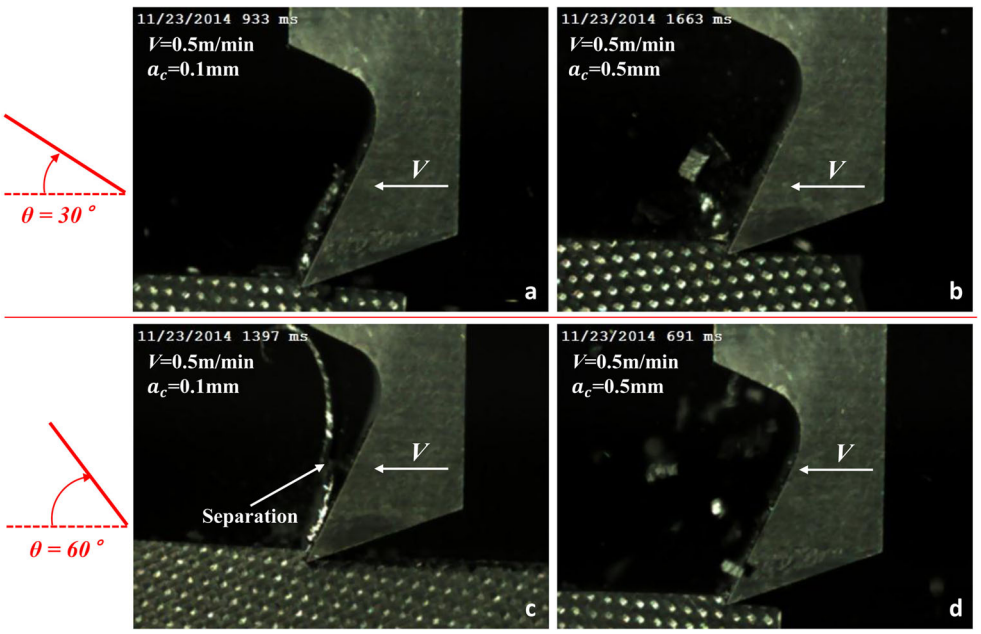

Fig. 4 Chip formation in UD-CFRP orthogonal cutting ($15° \leq \theta < 75°$)

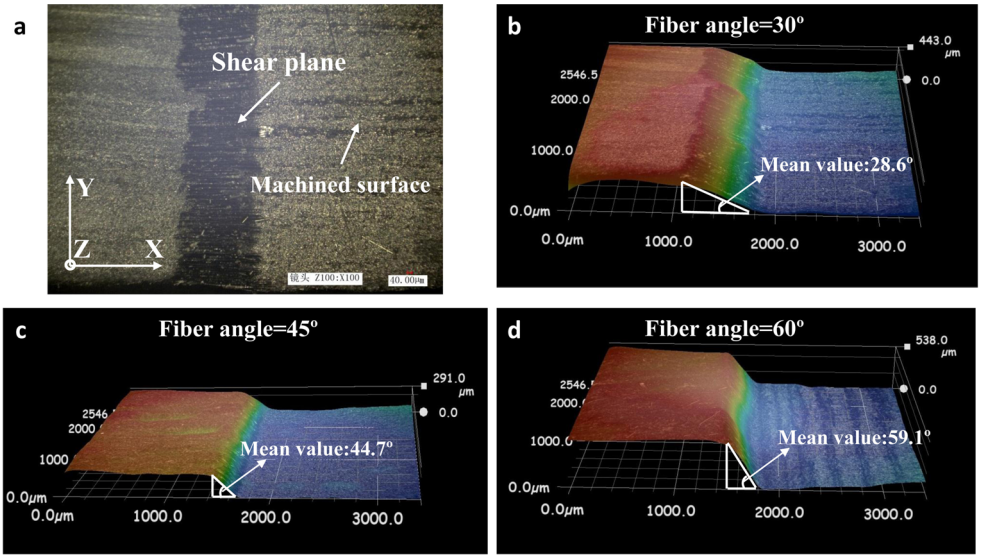

Fig. 5 Shear plane in UD-CFRP orthogonal cutting ($15° \leq \theta < 75°$)

where a_{ch} is the chip thickness, a_c is the DOC, V_c is the chip flow speed, and V is the tool cutting speed.

The fracture takes place at the point where the tool tip is in contact with the primary shear zone of the removed CFRP layer. The horizontal cutting force acting on the tool tip is the direct factor causing the removed layer to separate from the bulk material [27]. Consequently, the horizontal cutting force per unit width along the tool tip is equivalent to the material fracture toughness G_c, the value of which can be further regarded as surface energy. As a result, the remained horizontal force per unit width between tool and chip is $(F_c/a_w) - G_c$, where a_w is the cutting width. The force equation on the shear plane can be expressed as [28]

$$\frac{F_c}{a_w} - \frac{F_t}{a_w}\tan\phi = \tau_1 a_c \left(\tan\phi + \frac{1}{\tan\phi}\right) + G_c \tag{2}$$

where τ_1 is the shear strength of the workpiece along the fiber direction, F_c is the horizontal cutting force and F_t is the thrust force.

It is found that the shear plane exists along the fiber direction when $15° \leq \theta < 75°$. Chips are produced against the cutting tool by shearing of the fiber-matrix interface along

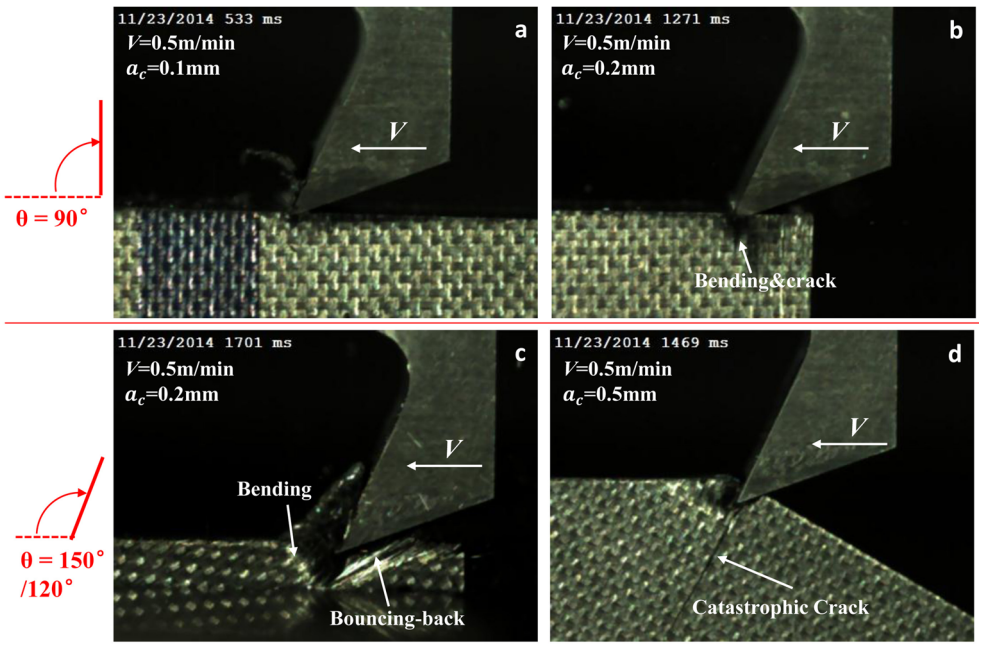

Fig. 6 Chip formation in UD-CFRP orthogonal cutting ($75° \leq \theta < 180°$)

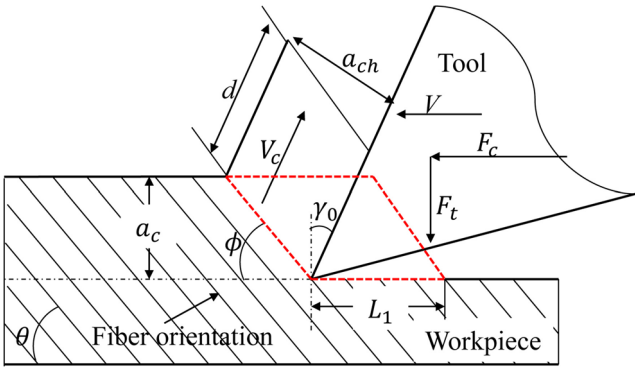

Fig. 7 Diagram of UD-CFRP orthogonal cutting model in the case of $75^\circ \leq \theta < 180^\circ$

the fiber direction, as elaborated in Section 3. Hence, the shear angle ϕ can be substituted by fiber angel θ and Eq. 3 giving

$$\frac{F_c}{a_w} - \frac{F_t}{a_w}\tan\theta = \tau_1 a_c\left(\tan\theta + \frac{1}{\tan\theta}\right) + G_c \tag{3}$$

Using the value of $\tan\theta$, the measured cutting force F_c, thrust force F_t, and subsequently the values of $F_c/a_w - (F_t/a_w)\tan\theta$ and $a_c(\tan\theta + 1/\tan\theta)$ under different DOCs and fiber angles can be calculated. Once $F_c/a_w - (F_t/a_w)\tan\theta$ versus $a_c(\tan\theta + 1/\tan\theta)$ is fitted into Eq. 3, the fracture toughness and shear strength of the workpiece can be obtained from the value of the vertical intercept and the slope of the fitted regression line.

According to the cutting process of CFRP orthogonal cutting, with cutting speed V, the increment of external work, E_{ext}, is given by $F_c V$. Under steady-state conditions, the energy remains unchanged and the following equation applies

$$E_{ext} = E_{diss} \tag{4}$$

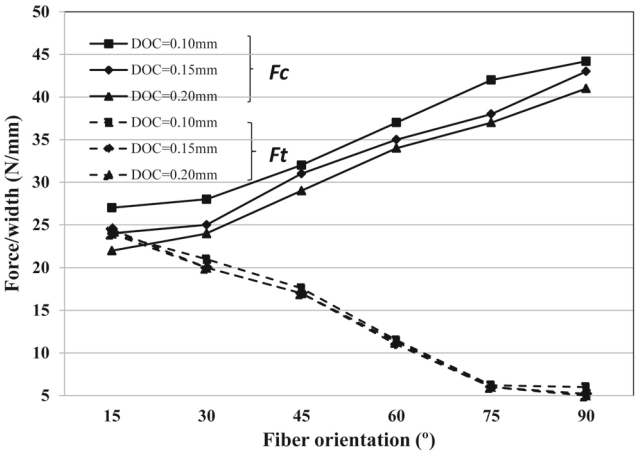

Fig. 8 Experimental results of the cutting forces (F/a_w) with the variation of fiber orientation

where E_{diss} is the increment of dissipated energy and can be given by,

$$E_{diss} = E_{fract} + E_{frict} + E_{chip} \tag{5}$$

where E_{fract}, E_{frict}, and E_{chip} are the fracture energy of new surface, frictional energy on the tool-chip interface, and chip fracture energy during the chip formation process, respectively. Thus, the energy required to form a new surface (i.e., the material fracture toughness G_c) is comparable with the energy consumed for plastic deformation and friction work and should not be ignored [28]. Hence, in this study, the new surface fracture energy is given by

$$E_{fract} = G_c a_w V \tag{6}$$

The friction force on the tool-chip interface is given by

$$S = (F_c - a_w G_c)\sin\gamma_0 + F_t\cos\gamma_0 \tag{7}$$

where γ_0 is the tool rake angle, and from Eq. 1, the friction energy on the tool-chip interface can be obtained by,

$$\begin{aligned} E_{frict} &= S \cdot V_c = S \cdot V \\ &= [(F_c - a_w G_c)\sin\gamma_0 + F_t\cos\gamma_0]V \end{aligned} \tag{8}$$

The chip morphology has been analyzed in Section 3 of this paper, and the chip removal mechanism is mainly interlaminar sliding along the fiber orientation θ. This fracture energy is the product of energy required for the formation of one fracture face and the number of fracture planes formed per unit time

$$E_{chip} = E_{fr}\frac{V}{d} \tag{9}$$

where d is the chip block thickness measured directly from CFRP orthogonal cutting process, which is illustrated in Fig. 7. E_{fr} is the fracture energy required for a single chip separation from a fracture plane

$$E_{fr} = G_c' A_{fr} \tag{10}$$

where G_c' is the chip surface energy which can also be called chip fracture toughness [29]. A_{fr} is the area of fracture in a shear plane, the fracture area, and can be expressed as $a_c a_w/\sin\phi$, and the chip fracture energy can be expressed as follows

$$E_{chip} = G_c' A_{fr} f = G_c'\frac{a_w a_c}{\sin\phi}\frac{V}{d} = G_c'\frac{a_w a_c}{\sin\theta}\frac{V}{d} \tag{11}$$

Therefore, the energy distribution on the four portions (i.e., plastic deformation, friction, new surfaces formation, and chip fracture) can be analyzed with Eq. 12.

$$\begin{aligned} F_c V &= G_c a_w V + [(F_c - a_w G_c)\sin\gamma_0 + F_t\cos\gamma_0]V \\ &\quad + G_c'\frac{a_w a_c}{\sin\theta}\frac{V}{d} \end{aligned} \tag{12}$$

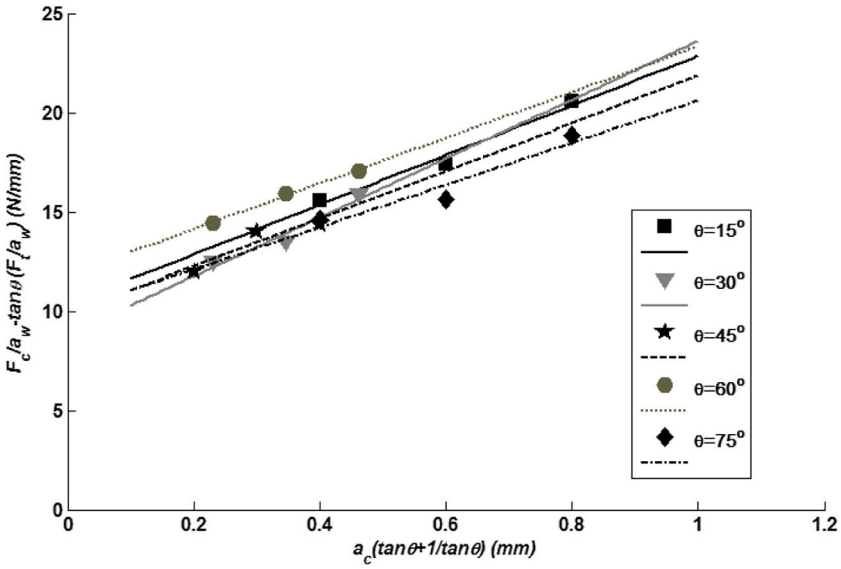

Fig. 9 Line fitting of $F_c/a_w - (F_t/a_w)\tan\theta$ vs. $a_c(\tan\theta + 1/\tan\theta)$, ($F_c$ cutting force, F_t thrust force, a_w cutting width, θ fiber angle, and a_c uncut chip thickness)

5 Results and discussion

5.1 Shear strength and fracture toughness

As shown in Fig. 8, the principle cutting force F_c increases with fiber orientation ($15° \leq \theta < 75°$) for different DOC selected. The thrust force F_t, however, is not sensitive to DOC and decreases with increasing θ. Combined with the measured results of cutting force F_c, thrust force F_t, and cutting parameters under the three different DOCs for each fiber orientation (15, 30, 45, 60, and 75°), five line-fittings between $F_c/a_w - (F_t/a_w)\tan\theta$ and $a_c(\tan\theta + 1/\tan\theta)$ are obtained based on Eq. 4, as shown in Fig. 9. The correlation coefficients (R^2 value) of the five lines are all greater than 0.93. The fracture toughness G_c and the shear strength τ_1 of the workpiece material with five different θ can then be determined from the vertical intercepts and the slopes of these fitted lines. The calculation results of G_c and τ_1 for different is shown in Table 3.

From Table 3, it can be found that the shear strength along fiber direction is independent on fiber angle. The mean value of shear strength is 12.290 MPa, whereas the experimental measurements of fiber-matrix interface shear strength is 15–25 MPa [30], the variation might be due to error in cutting force measurements and the effect of cutting edge radius. The fracture toughness of new machined surface G_c of different fiber orientations are also shown in Table 3. No obvious change in G_c can be found with increasing fiber angle; the mean value will be used for energy conservation calculation in the following section.

Table 3 Results of shear strength and fracture toughness under different fiber angles

$\theta(°)$	15	30	45	60	75	Mean value
τ_1 (Mpa)	12.5	14.8251	12	11.4932	10.634	12.290
$G_c(KJ/m^2)$	10.3597	8.7914	9.8667	11.8374	9.9785	10.166

5.2 Energy distribution in CFRP orthogonal cutting

The chip surface energy G_c' under different cutting conditions can be obtained through polynomial operation of Eq. 12. The energy consumed during the cutting process is attributed to new surface energy, friction, and chip fracture energy. Figure 10 shows the energy distribution on these three factors for fiber angles 30, 45, and 60°, respectively. When the fiber angle is 30°, the energy spent on the new machined surface accounts for 32.36 %, the energy for the friction accounts for 51.14 %, while the energy spent on the chip fracture accounts for 16.5 %. It can be found that the new surface energy in CFRP

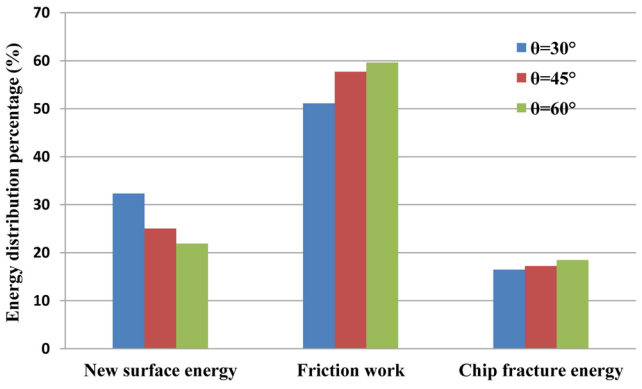

Fig. 10 Effect of fiber angle on the energy distribution in CFRP cutting process (cutting speed: 0.5 m/min, DOC: 0.1 mm, and rake angle: 5°)

orthogonal cutting tends to decrease with increasing θ. For all three fiber orientations, the energy consumed in tool-chip friction is the greatest, and its value increases with increasing θ. This might be caused by the increasing friction coefficient at the interface of tool-chip for different θ.

6 Conclusions

In this work, a new approach is proposed for predicting UD-CFRP fracture toughness based on the William model. Energy conservation analysis is carried out which considers the energy consumption for creating new machined surface. The fracture toughness of separation between segments in block chips in CFRP orthogonal cutting process has also been discussed. The following conclusions are drawn:

1. Both fiber orientation θ and DOC have strong influence on the chip formation mechanism and chip morphology. The chips are powder-like or ribbon-like, when the DOC is small ($\leq$0.1 mm in this paper), but become blocky with increasing DOC.
2. In the case of $15° \leq \theta < 75°$, chips are produced by the matrix-fiber interface shearing along the fiber direction, and when the fiber angle is over 75°, the chip is yielded due to bending fracture and might lead to the fiber bouncing-back in the cutting process, and this would degrade the surface roughness of machined surface.
3. The fracture toughness and shear strength of the workpiece material can be determined from line fitting of $F_c/a_w-(F_t/a_w)\tan\theta$ and $a_c(\tan\theta+1/\tan\theta)$ when the fiber orientation θ is between 15 and 75°; the fracture toughness of new machined surface G_c is independent of θ.
4. The energy consumption during the CFRP machining process consists of three factors (new surface energy, friction, and chip fracture energy) and the tool-chip friction energy plays a predominant role, then is new surface energy and chip fracture energy. Energy consumption for creating new machined surface decreases with increasing θ.

This work provides new insights into the machining process of CFRP, which may in turn help to improve the composite machining process quality control.

Acknowledgments The authors would like to acknowledge the financial support by National Natural Science Foundation of China (Grant No. 51275345 and 51420105007), and National NC Science and Technology Major Projects (Grant No. 2014ZX04001081).

References

1. Chibane H, Morandeau A, Serra R, Bouchou A, Leroy R (2013) Optimal milling conditions for carbon/epoxy composite material using damage and vibration analysis. Int J Adv Manuf Technol 68(5-8):1111–1121
2. Silva D, Teixeira JP, Machado CM (2014) Methodology analysis for evaluation of drilling-induced damage in composites. Int J Adv Manuf Technol 71(9-12):1919–1928
3. Qi Z, Zhang K, Cheng H, Wang D, Meng Q (2015) Microscopic mechanism based force prediction in orthogonal cutting of unidirectional CFRP. Int J Adv Manuf Technol:1–11
4. Arul S, Vijayaraghavan L, Malhotra S, Krishnamurthy R (2006) The effect of vibratory drilling on hole quality in polymeric composites. Int J Mach Tools Manuf 46 (3):252–259
5. Davim JP, Reis P (2003) Drilling carbon fiber reinforced plastics manufactured by autoclavełexperimental and statistical study. Mater Design 24(5):315–324
6. Soussia AB, Mkaddem A, El Mansori M (2014) Rigorous treatment of dry cutting of FRP-Interface consumption concept: a review. Int J Mech Sci 83:1–29
7. Singh I, Bhatnagar N (2006) Drilling of uni-directional glass fiber reinforced plastic (UD-GFRP) composite laminates. Int J Adv Manuf Technol 27(9-10):870–876
8. Arul S, Vijayaraghavan L, Malhotra S, Krishnamurthy R (2006) The effect of vibratory drilling on hole quality in polymeric composites. Int J Mach Tools Manuf 46(3):252–259
9. Komanduri R (1997) Machining of fiber-reinforced composites. Mach Sci Technol 1(1):113–152
10. Koplev A, Bunsell A (1980) Machining of fiber-reinforced composites. In: 3rd International Conference of Advances in Composite Materials, pp 1597–1605
11. Arola D, Ramulu M, Wang D (1996) Chip formation in orthogonal trimming of graphite/epoxy composite. Compos Part A-Appl S 1(1):113–152
12. Nayak D, Bhatnagar N, Mahajan P (2005) Machining studies of uni-directional glass fiber reinforced plastic (UD-GFRP) composites part 1: effect of geometrical and process parameters. Mach Sci Technol 9(4):481–501
13. Zitoune R, Collombet F, Lachaud F, Piquet R, Pasquet P (2005) Experiment-calculation comparison of the cutting conditions representative of the long fiber composite drilling phase. Compos Sci Technol 65(3):455–466
14. Zhou L, Hou N, Huang S, Xu L (2014) An experimental study on formation mechanisms of edge defects in orthogonal cutting of SiCp/Al composites. Int J Adv Manuf Technol 72(9-11):1407–1414
15. Everstine G, Rogers T (1971) A theory of machining of fiber-reinforced materials. J Compos Mater 5(1):94–106
16. Bhatnagar N, Ramakrishnan N, Naik N, Komanduri R (1995) On the machining of fiber reinforced plastic (FRP) composite laminates. Int J Mach Tools Manuf 35(5):701–716
17. Zhang L, Zhang H, Wang X (2001) A force prediction model for cutting unidirectional fibre-reinforced plastics. Mach Sci Technol 5(3):293–305
18. Jahromi AS, Bahr B (2010) An analytical method for predicting cutting forces in orthogonal machining of unidirectional composites. Compos Sci Technol 70(16):2290–2297
19. Ernst H, Merchant ME (1941) Chip formation, friction and finish. Cincinnati milling machine Company
20. Rahamathullah I, Shunmugam M (2014) Mechanistic approach for prediction of forces in micro-drilling of plain and glass reinforced epoxy sheets. Int J Adv Manuf Technol 75 (5-8):1177–1187

21. Atkins A (2003) Modelling metal cutting using modern ductile fracture mechanics: quantitative explanations for some longstanding problems. Int J Mech Sci 45(2):373–396
22. Astakhov VP, Xiao X (2008) A methodology for practical cutting force evaluation based on the energy spent in the cutting system. Mach Sci Technol 12(3):325–347
23. Williams J, Patel Y, Blackman B (2010) A fracture mechanics analysis of cutting and machining. Eng Fract Mech 77 (2):293–308
24. Wang X, Zhang L (2003) An experimental investigation into the orthogonal cutting of unidirectional fibre reinforced plastics. Int J Mach Tools Manuf 43(10):1015–1022
25. Rao GVG, Mahajan P, Bhatnagar N (2007) Machining of UD-GFRP composites chip formation mechanism. Compos Sci Technol 67(11):2271–2281
26. Ramulu M, Kim D, Choi G (2003) Frequency analysis and characterization in orthogonal cutting of glass fiber reinforced composites. Compos Part A-Appl S 34(10):949–962
27. Patel Y, Blackman B, Williams J (2009) Determining fracture toughness from cutting tests on polymers. Eng Fract Mech 76(18):2711–2730
28. Wang B, Liu Z, Yang Q (2013) Investigations of yield stress, fracture toughness, and energy distribution in high speed orthogonal cutting. Int J Mach Tools Manuf 73:1–8
29. Shet C, Chandra N (2002) Analysis of energy balance when using cohesive zone models to simulate fracture processes. J Eng Mater Technol 124(4):440–450
30. Rao GVG, Mahajan P, Bhatnagar N (2007) Micro-mechanical modeling of machining of FRP composites-Cutting force analysis. Compos Sci Technol 67(3-4):579–593